NTNU

Norwegian University of
Science and Technology

# Valence excitation energies in multilevel coupled cluster

Jon Espen Jensen

Master of Science
Submission date: June 2017
Supervisor: Ida-Marie Høyvik, IKJ

Norwegian University of Science and Technology
Department of Chemistry

# Abstract

This is a benchmark study, for valence excitation energies in the multilevel coupled cluster (MLCC) framework. The information resulting from lower level of theory is used to generate correlated natural transition orbitals (CNTOs) for the high level calculations by including the information from both the singles and the doubles excitation vectors. The CNTOs are included in the active space according to certain thresholds corresponding to the eigenvalues of the orbitals. The MLCC results for valence excitation energies in the inactive space are calculated using coupled cluster singles and doubles (CCSD), and the active space are calculated using CCSD with perturbative triples (CC3). The errors relative to full CC3 depends on the thresholds. In general to obtain errors less than 10% on needs to include approximately 60-70% of the orbital space for the investigated molecules.

# Sammendrag

Dette er en benchmark studie, for valens eksitasjons energier i *multilevel coupled cluster* (MLCC) rammeverket. Informasjonen som er oppnådd fra lavere grads teori er brukt til å generere *correlated natural transition orbitals* (CNTOs) for høyere grads beregninger ved å inkludere informasjon fra både de enkle og doble eksitiasjons vektorene. CNTO'ene inkluderes i det aktive rommet innenfor et sett av thresholds som korresponderer til egenverdiene til orbitalene. MLCC resultatene for valens eksitasjons energiene i det inaktive rommet beregnes med *coupled cluster singles and doubles* (CCSD), og det aktive rommet beregnes med CCSD med perturbative tripletter (CC3). Feilene sammenlignet med full CC3 er avhengig av hvilke thresholds som brukes. Generelt for å oppnå feil mindre enn 10% må det inkluderes 60-70% av orbitalrommet for de undersøkte molekylene.

# Acknowledgments

First I would like to thank my supervisor, Assoc. Prof. Ida-Marie Høyvik, for regular meetings, support and help throughout this project. She gave me exactly the opportunity i needed during my educations darkest hour, and because of her showing such an example and dedication, she went on to relight a fire in me, and i am forever grateful to her for everything that she has done for me. A big thank you aswell to Prof. Henrik Koch who also offered suprivison og help during this project.

Thank you to the other master students for their cooperation and support. Gratitude to all of my friends and all friends i've made on this extraordinary journey. And at last a big thank you to my parants for financial and moral support. I'd like to end this chapter of my life with the words of a wise man who once said *"one journey ends, as another begins"*, so I am now very much looking forward to the opportunity of practising the art of teaching on a full time basis.

# Contents

# Abbreviations

| | |
|---|---|
| **AO** | **A**tomic **O**rbital |
| **aug-cc-pVXZ** | augmented correlation consistent |
| **CBS** | **C**omplete **B**asis **S**et |
| **CC** | **C**ouple **C**luster |
| **cc** | **c**orrelation **c**onsistent |
| **CI** | **C**onfiguration **I**nteraction |
| **CCSD** | **C**ouple **C**luster **S**ingles and **D**oubles |
| **CCSDT** | **C**ouple **C**luster **S**ingles, **D**oubles and **T**riples |
| **CNTOs** | **C**orrelated **N**atural **T**ransition **O**rbitals |
| **CT** | **C**harge **T**ransfer |
| **DZ** | **D**ouble **Z**eta |
| **FCI** | **F**ull **C**onfiguration **I**nteraction |
| **GTO** | **G**aussian **T**ype **O**rbitals |
| **HF** | **H**artree -**F**ock |
| **HOMO** | **H**ighest energy **O**ccupied **M**olecular **O**rbital |
| **LUMO** | **L**owest energy **U**noccupied **M**olecular **O**rbital |
| **MLCC** | **M**ulti- **L**evel **C**ouple **C**luster |
| **MLCC3** | **M**ulti- **L**evel **CC3** |
| **MO** | **M**olecular **O**rbital |
| **MPPT** | **M**öller **P**lesset**P**erturbation**T**heory |
| **MP2** | **S**econd **O**rder **M**öller **P**lesset **P**erturbation |
| **NTOs** | **N**atural **T**ransition **O**rbitals |
| **SCF** | **S**elf **C**onsistent **F**ield |
| **STO** | **S**later **T**ype **O**rbitals |
| **TZ** | **T**riple **Z**eta |

*"Do not go were your path may lead, go instead where there is no path and leave a trail"*

RALPH WALDO EMERSON

# Chapter 1

# Introduction

Coupled cluster (CC) has proven to be a successful model of electronic wave function theory in terms of giving an accurate description of the molecular systems and it also gives a systematic framework for calculating molecular properties such as excitation energies accurately. The coupled cluster model where the singles and doubles excitation operators are included is called coupled cluster singles and doubles (CCSD). And the CC model where the singles, doubles and triples excitation operators are included is called called coupled cluster singles, doubles and triples (CCSDT) and so on. This constitutes the CC-hierarchy [7]. Furtermore approximative models have been developed for each of these truncated CC models, where the CC2 model is an approximative model of CCSD, and CC3 and CCSD(T) are approximative models of the CCSDT model [30]. However, one of the drawbacks of the CC hierarchy is the computational scaling with system size, and over the years much research has gone into developing CC models with reduced computational scaling [15, 20, 28]. One way of accomplishing reduced computational scaling is exploiting the locality of electron correlation, and a number of steps in this direction has been taken and seen further developments [13, 23, 29]. One of these resulting steps would be the development of the multilevel couple cluster model (MLCC), where a specific area of the molecule is treated with high level of theory and the rest of the molecule is treated with lower level of theory [25, 30].

Pulay and Sæbø laid the foundation of local correlation methods [31], and also an important early contribution were presented by Werner et al. in terms of developing a local coupled cluster method [32]. There are also other ways of attempting to reduce the scaling in correlation methods. Such methods include atomic orbital based CC [11], the natural linear scaling approach [14], local CC using bump functions [34]. These methods use local occupied HF orbitals, but they have not been able to apply local virtual HF orbitals, and as a consequence projected atomic orbitals (PAOs) are used instead. An alternative which have been presented to local correlation methods have been to parallize the CC method over multiple nodes [9]. This has become a useful tool due to the advancements in supercomputers, but it does not overcome the scaling obstacle.

A number of molecular properties are size-intensive, and size-intensive means that the properties depend only upon a specific area of the molecule. This is the fundamental idea behind multilevel CC methods, where high level computation is carried out on a certain area of the molecule, and the rest of the molecule is computed with lower level of theory. This procedure is done by seperating the orbital space into two (or more) subspaces, where each subspace is associated with an excitation manifold [25, 30]. In recent years the orbital space in multilevel CC-theory has been divided in two, where the atoms in the molecule and their corresponding atomic orbitals (AOs) are classified as either active or inactive. And Cholesky decomposition of the diagonal elements of the Hartree Fock (HF) density matrix has been used to determine the active and inactive spaces [30].

Excitation energies are used by experimentalists in spectroscopic techniques such as X-ray absorption spectroscopy and UV-vis absorption spectroscopy [27]. The concept in absorption spectroscopy is that a beam of radiation is focused on a sample and then the absorption of the radiation as a function of the frequency or wavelength is measured due to the interaction with the sample. The intensity varies as a function of the frequency, and this then constitutes the absorption spectrum. An excitation energy refers to the energy required for an electronic

transition from one orbital to another, where each orbital has a specific energy level [27]. We will consentrate on the five lowest valence excitation energies, and each of these energies would correspond to a specific peak in the absorption spectrum. Absorption spectroscopy is essential to identify electronic and molecular properties such as charge transfer, nature of bonding, hybridization, chemical environment and site symmetry [12].

In recent time, CC models using natural transition orbitals (NTOs) have been developed for calculating electronic transitions efficiently. Luzanov et al [24] introduced NTOs as a compact orbital representation for the transition density matrix. Furthermore as an example Baudin and Kristensen [8] use NTOs in combination with local occupied orbitals and local virtual orbitals for the purpose of generating a reduced orbital space specific to a particular transition where a CC calculation is carried out. The orbital space is further optimized to make certain that the excitation energies that are obtained are determined within a predefined precision [8]. We use a black box procedure, as described by Høyvik, Koch and Myhre [15], for obtaining the active space in our multilevel CC calculations by including the information obtained from the double excitation vector. The single and double excitation information are obtained from the lower level of theory and then used to tailor an active orbital space for the high level calculation. These resulting orbitals are referred to as correlated natural transition orbitals (CNTOs). The eigenvalues corresponding to the CNTOs provide a way of determining which orbitals that should be included in the active space through a set of thresholds for the occupied and virtual orbital space. In the limit of the thresholds equal to zero, the full orbital space is included in the active space, which means the entire molecular system is then treated with high level of theory [15].

In this project valence excitation energies are studied, which are particularly used in UV-vis absorption spectroscopy. The CNTOs are used within certain sets of thresholds to calculate these valence excitation energies in the MLCC framework and compared with valence excitation energies calculated with the full CC3 model.

# Chapter 2

# Theory

## 2.1 The Schrödinger equation

The Born-Oppenheimer approximation says that because the nucleus is so much heavier then the electrons moving around it, then the nucleus can be treated as stationary with respect to the electrons moving around it. So the non-relativistic time-independent Schrödinger equation, within the Born-Oppenheimer approximation, can be expressed as the following equation [7]

$$H|\Psi\rangle = E|\Psi\rangle \tag{2.1}$$

where $|\Psi\rangle$ is the exact electronic wavefunction describing the system, E is the energy, and H is the hamilton operator. The hamilton operator (here represented in atomic units) can be expressed as

$$H = -\frac{1}{2}\sum_{i}^{N_e}\nabla_i^2 - \sum_{i}^{N_e}\sum_{I}^{N_n}\frac{Z_I}{|r_i - R_I|} + \frac{1}{2}\sum_{i\neq j}^{N_e}\frac{1}{|r_i - r_j|} + \sum_{I\neq J}^{N_n}\frac{Z_I Z_J}{|R_I - R_J|} \tag{2.2}$$

where $N_e$ is the number of electrons, $N_n$ is the number of nuclei, $Z_I$ is the atomic number of nucleus I, $R_I$ is the coordinates of nucleus I, and $r_i$ is the coordinates of electron i. $\nabla_i^2$ is the Laplace operator which is defined as

$$\nabla_i^2 = \left( \frac{\partial^2}{\partial x_i^2} + \frac{\partial^2}{\partial y_i^2} + \frac{\partial^2}{\partial z_i^2} \right) \tag{2.3}$$

With regards to the Schrödinger equation, it can only be solved analytically for one-electron systems, but for larger systems approximative methods would have to be used when solving the Schrödinger equation. While approximative methods are unable to solve the problem accurately the solutions given will have a given accuracy. However for larger systems, the exact solution within a given one-electron basis can be obtained by full configuration interaction (FCI), which can be represented as a linear combination of all determinants as expressed by the following equation

$$|FCI\rangle = \sum_{M=1}^{D} C_M |M\rangle \tag{2.4}$$

The expansion coefficients, $C_M$, are found by using the variational principle. The variational principle states that by choosing a "trial wavefunction, $(\Psi_{trial})$" defined as

$$\Psi_{trial} = \sum_{I=1}^{D} C_I \Phi_I \tag{2.5}$$

that gives an expectation value for the energy that is as low as possible according to the variational theorem that says:

$$\frac{< \Psi_{trial} | \hat{H} | \Psi_{trial} >}{< \Psi_{trial} | \Psi_{trial} >} \geq E_0 \tag{2.6}$$

Where $E_0$ is the exact energy to the groundstate and the equality only holds if the trial wavefunction is identical to the exact wavefunction for the groundstate. The variational principle then states that the approximated energy found, is always larger or equal to the exact energy $(E_0)$ [7].

The number of determinants, D, has a factorial dependency with respect to the number of spin orbitals, and the number of coefficients depend on the number of electrons and the number of spin orbitals according to the binomial distribution as follows

$$NC_n = \frac{N!}{n!(N-n)!} = \begin{pmatrix} \text{N} \\ \text{n} \end{pmatrix} \tag{2.7}$$

Where $NC_n$ represents the number of determinants for n-electrons and N spin-orbitals, this makes the FCI model practically impossible to use on anything other then small systems [35].

## 2.2 Hartree-Fock Theory

Hartree Fock [7] is based upon the variatonal principle, and also upon the assumption that every electron moves in an average electrostatic field with respect to the other $N_e - 1$ electrons. HF is method in attempting to solve the schrödinger equation, where the Hamiltonian can be seperated into a sum of one-electron hamiltonians ($h_i$) for every electron, i, according to the following formula

$$\hat{H} = \sum_{i}^{n} \hat{h_i} \tag{2.8}$$

But to satisfy the Pauliprinciple, which states that the total wavefunction must be antisymmetric, it is written as a determinant

$$\Psi = \frac{1}{\sqrt{N_e!}} det|\varphi_1(1)\varphi_2(2)...\varphi_{N_e}(N_e)| \tag{2.9}$$

Where $\varphi(i) = \varphi_i(\overrightarrow{r}_i)\sigma(m_s)$, and the spatial part is given by a linear combination of atomic orbitals (AOs), $\varphi_i = \sum_\mu C_{\mu i}\chi_\mu$.
In order to find the lowest energy, the variational principle and Lagrange multipliers method

is applied on the expectation value for the energy, ($E = \frac{<\psi_{trial}|H|\psi_{trial}>}{<\psi_{trial}|\psi_{trial}>}$), and then differentiate with respect to the MO-coefficients. This leads to the following matrix equation

$$\mathbf{FC} = \varepsilon\mathbf{SC} \tag{2.10}$$

Where C is a matrix containing the MO-coefficients, S is the overlap matrix of AOs, $\varepsilon$ is a matrix containing all the orbital energies, and F is the Fock matrix. The F matrix contains integrals where the fockoperator for every electron acts on the atomic orbital for the respective electron. To illustrate this for electron 1, then the equation that must be solved is

$$\hat{f}_1\varphi_a(1) = \varepsilon_a\varphi_a(1) \tag{2.11}$$

Where $\hat{f}_1$ is the fockoperator for electron 1, defined by the Coulumb operator, $\hat{J}_m$, and the exchange operator, $\hat{K_m}$, and the hamiltonian for electron 1, where $j_0 = \frac{e^2}{4\pi\varepsilon_0}$, according to the following equations

$$\hat{F} = \sum_{i=1}^{N_e} \hat{f}_i \tag{2.12}$$

$$\hat{f}_1 = \hat{h_1} + \sum_m [2\hat{J_m}(1) - \hat{K_m}(1)] \tag{2.13}$$

$$\hat{J}_m(1)\varphi_a(1) = j_0 \int \varphi_m^*(2)\frac{1}{r_{12}}\varphi_a(1)\varphi_m(2)d\tau_2 \tag{2.14}$$

$$\hat{K}_m(1)\varphi_a(1) = j_0 \int \varphi_m^*(2)\frac{1}{r_{12}}\varphi_m(1)\varphi_a(2)d\tau_2 \tag{2.15}$$

So in order to solve eq 2.10 in practice, this is done iteratively, which means a set

of MO-coefficients is guessed through a self consistent field (SCF) procedure, where the MO-coefficients is first guessed and then equation 2.10 is solved iterativley until matrix C converges [7, 35].

## 2.3 Electron correlation

Electron correlation [35] is defined as the difference between the exact energy, i.e., the energy obtained by Full Configuration Interaction (FCI), and the HF energy, as shown in eq 2.16, this energy corresponds to the motion of correlated electrons.

$$E_{corr} = E_{exact} - E_{HF} \tag{2.16}$$

However practically we can only calculate these energies within a given basis, which is why in a practical manner, the equation for electron correlation becomes:

$$E_{corr}^{basis} = E_{exact}^{basis} - E_{HF}^{basis} \tag{2.17}$$

Hartree-Fock is a model where the physical interpretation is that every electron moves in an average electrostatic field with respect to the other $N_e - 1$ electrons. But looking at the movement of the electrons in an average way is not good enough. Electron Correlation arises from the desire to describe the detailed correlated motion of electrons as induced by their instantaneous mutual repulsion. Because of the Variational principle that says the HF energy will always be higher then the exact energy, then as a consequence the correlation energy will be negative, $E_{corr} < 0$. Electron correlation can be divided into two types of correlation, dynamic and static correlation. Dynamic correlation is associated with capturing the effect of instantaneous electron repulsion, such as for those electrons occupying the same spatial orbital and thus have opposite spin. Static correlation is associated with small differences in energy between different states and where more than one determinant is required to cover the electronic structure. To describe static correlation models such as Multi-Configurational

Self Consistent field (MCSCF), or other multi-reference methods, would have to be used. But a model such as Coupled Cluster does a good job of describing dynamic correlation [35].

## 2.4 Møller-Plesset Second Order Correction (MP2)

An important observation is that Møller Plesset with first order correction is equivalent to Hartree Fock because of the following relation

$$E_{HF} = E_0^{(0)} + E_0^{(1)} \tag{2.18}$$

However Møller Plesset that also includes second order correction is denoted as MP2, and the energy expression for MP2 will then be

$$E_{MP2} = E_0^{(0)} + E_0^{(1)} + E_0^{(2)} = E_{HF} + E_0^{(2)} \tag{2.19}$$

Where $E_0^{(2)}$ is given as

$$E_0^{(2)} = -\frac{1}{4} \sum_{ijab} \frac{|\langle ij||ab\rangle|^2}{\varepsilon_a + \varepsilon_b - \varepsilon_i - \varepsilon_j} \tag{2.20}$$

It is important to point out that the second order correction to the energy will always give a negative contribution to the energy.

MP2 is a very simple model with a very low computational cost which include electron correlation. It is said that MP2 recover as much as 80-90% of the electron correlation [17]. In this thesis the MP2 method was only used for geometry optimization as also stated in section 4.1.

## 2.5 Coupled Cluster Theory

The fundamental idea in Coupled Cluster theory [7] is that the exact electronic wavefunction ($\Psi$) is related to a reference-wavefunction ($\Phi_0$) through an exponential operator, $e^{\hat{T}}$, where $\hat{T}$ is the Cluster operator, and the reference wavefunction is usually the Hartree-Fock wavefunction ($\Phi_{HF}$). This is shown through the following equations:

$$|\Psi >= e^{\hat{T}}|\Phi_{HF} > \tag{2.21}$$

$$e^{\hat{T}} = 1 + \hat{T} + \frac{1}{2!}\hat{T}^2 + \frac{1}{3!}\hat{T}^3 + ... = \sum_{n=0}^{\infty} \frac{1}{n!}\hat{T}^n \tag{2.22}$$

The effect of the operator $\hat{T}$ is the sum of the effect of the one-electron excitation operator $\hat{T}_1$, the two-electron excitation operator $\hat{T}_2$, and all the way up to the N-electron excitation operator $\hat{T}_N$:

$$\hat{T} = \hat{T}_1 + \hat{T}_2 + \hat{T}_3 + .. + \hat{T}_N \tag{2.23}$$

The effects of the excitation operators are:

$$\hat{T}_1|\Phi_{HF} >= \sum_{ia} t_i^a|\Phi_i^a > \tag{2.24}$$

$$\hat{T}_2|\Phi_{HF} >= \sum_{ijab} t_{ij}^{ab}|\Phi_{ij}^{ab} > \tag{2.25}$$

And likewise for $\hat{T}_3$ all the way up to $\hat{T}_N$. Where $t_i^a$ is the single excitation amplitude, and $t_{ij}^{ab}$ is the double excitation amplitude etc. CC is equivalent to FCI when the clusteroperator $\hat{T}$ contains all $\hat{T}_1$ to $\hat{T}_N$ where n is the number of electrons in the system. The clusteroperator is, in the case of FCC, equivalent to that of equation 2.23, but the clusteroperator, in the case

of truncated CC, contains only specific exitation operators. For example the clusteroperator for CCSD is $\hat{T} = \hat{T}_1 + \hat{T}_2$, and for CCSDT then $\hat{T} = \hat{T}_1 + \hat{T}_2 + \hat{T}_3$ etc.The CC wave function for a given orbital basis satisfies the Schrödinger equation

$$\hat{H} \exp(\hat{T})|\Phi_{HF}> = \ E \exp(\hat{T})|\Phi_{HF}> \tag{2.26}$$

CC is not a variational method, so the energy and the amplitudes are determined rather by subspace projections than by using the variational theorem. This is done by multiplying eq. 2.26 from the left with $exp(-\hat{T})$. The subspace projections are carried out with respect to the HF state, $\langle\Phi_{HF}|$, and the excited state determinants, $\langle\mu|$, which gives the following equations for the energy and the amplitudes

$$\langle\Phi_{HF}| \exp(-\hat{T})\hat{H} \exp(\hat{T})|\Phi_{HF}\rangle = E \tag{2.27}$$

$$\langle\mu| \exp(-\hat{T})\hat{H} \exp(\hat{T})|\Phi_{HF}\rangle = 0 \tag{2.28}$$

CC unlike HF is not variational, but CC is size-consistent. An important point regarding the CC-method is that it is a post HF-method. It relieves some of the problems in the HF-method due to electron correlation as shown in eq. Furthermore the CC-method is only capable of giving a good description of dynamic correlation, but CC does not give a good description of static correlation.

Another point is that CC is a size-extensive method, meaning that energies calculated vary linearly with respect to the number of particles when the system size increases. As mentioned earlier CC, unlike HF, is not a variational method, and as a consequence the resulting

electronic energy may be lower than the true energy.

$$E_{CC} = E_{HF} + E_{corr} \tag{2.29}$$

The standard CC models are expressed in terms of delocolized CMO's, resulting in steep computational scaling, meaning that they can only be used on small molecular systems. However electron correlation is an example of a local effect, and for those effects that are local, the scaling may be bypassed by expressing the correlated wavefunction in terms of a set of local HF orbitals.

### 2.5.1 CC3

The CC3 model [10] and the CCSD(T) model are both approximations to the CCSDT model. The advantage is that both CC3 and CCSD(T) shows a reduction in scaling, $N^7$ as opposed to $N^8$, compared to CCSDT. The CCSDT state is defined as

$$|CCSDT\rangle = exp(\hat{T}_1 + \hat{T}_2 + \hat{T}_3)|HF\rangle \tag{2.30}$$

The cluster amplitudes are determined by projecting the schrödinger equation onto the space of single, double and triple excitations from the HF reference state, where $i = 1, 2, 3$. In order to determine the CCSDT state the following equations must be solved

$$\langle \mu_i | exp(-\hat{T}_1 - \hat{T}_2 - \hat{T}_3)\hat{H}exp(\hat{T}_1 + \hat{T}_2 + \hat{T}_3)|HF\rangle = 0 \tag{2.31}$$

Presenting a $t_1$-similarity transformation, $\tilde{O} = exp(-\hat{T_1})\hat{O}exp(\hat{T_1})$, and the hamiltonian, $\hat{H}$ then becomes

$$\tilde{H} = exp(-\hat{T_1})\hat{H}exp(\hat{T_1}) \tag{2.32}$$

The singles and doubles equation for both CC3 and CCSDT are as follows

$$\left\langle \mu_1 | [\tilde{H}, \hat{T_2}] | HF \right\rangle + \left\langle \mu_1 | [\tilde{H}, \hat{T_3}] | HF \right\rangle = 0 \tag{2.33}$$

$$\left\langle \mu_2 | \tilde{H} + [\tilde{H}, \hat{T_2}] + \frac{1}{2}[[\tilde{H}, \hat{T_2}], \hat{T_2}] | HF \right\rangle + \left\langle \mu_2 | [\tilde{H}, \hat{T_3}] | HF \right\rangle = 0 \tag{2.34}$$

Without external perturbations the equation determining the triples is

$$\left\langle \mu_3 | \hat{F}, \hat{T_3}] | HF \right\rangle + \left\langle \mu_3 | [\hat{U}, \hat{T_3}] | HF \right\rangle = 0 \tag{2.35}$$

Equations 2.33, 2.34, 2.35 define the CC3 energy in a system where there are no external perturbations. The single and double excitations are included to an infinite order and the triple excitations are determined pertubatively.

The Hamiltonian can be partitioned into two terms, the Fock operator ($\hat{F}$) and the fluctuation potential ($\hat{U}$).

$$\hat{H} = \hat{F} + \hat{U} \tag{2.36}$$

There are no approximations with regards to the treatment of single excitations, this is because they act as orbital relaxation parameters. This results in the single amplitude being treated to zeroth order in the fluctuation potential, while the triple excitations are treated correctly to the second order. As mentioned before the CC3 model is a good approximation to the CCSDT model as it reduces the computational scaling from $N^8$ to $N^7$. The CC3

model then scales to the same order as CCSD(T), and CC3 has the same accuracy and robustness as CCSD(T), however CC3 preforms better for calculations of time-independent properties [10, 19].

### 2.5.2 Multi-level Coupled Cluster

The essential idea in the multi-level Coupled Cluster (MLCC) method is dividing the molecular system into different subsspaces, and these subspaces are treated with different levels of the CC hierarchy. For example in the MLCC3 model approach, the CC3 model is used to describe the active part of the molecule and CCSD model is used for the rest of the molecule. This approach then results in reduction in computational cost by treating the most important part of the system with higher level of accuracy. A way of partitioning the system is to divide it into an active and an inactive space, this can be done by assigning the highest occupied molecular orbital (HOMO) and the lowest unoccupied molecular orbital (LUMO) to the active space. Other ways of partitioning the system into active and inactive spaces is by using Cholesky decomposition. Since MLCC3 treats only a small part of the molecule with CC3, and the rest with CCSD, the computational scaling will be equal to CCSD, but the accuracy is comparable to CC3 [25, 30]. Which is something that will be investigated in this thesis, where valence excitation energies for different molecules computed by MLCC3 will be compared to the valence excitation energies computed with CC3.

MLCC is not so different from active space CC presented by Olsen and Köhn [21, 26], but the difference is that MLCC can include several levels of theory, making it possible for MLCC to gradually increase accuracy. In MLCC the Cluster operator, $\hat{T}$, is partitioned into $\hat{X} + \hat{S}$, resulting in the following equation

$$|CC\rangle = \exp(\hat{T})|\Phi_{HF}\rangle = \exp(\hat{X} + \hat{S})|\Phi_{HF}\rangle \tag{2.37}$$

Both of the operators, $\hat{X}$ and $\hat{S}$, are associated with the subspace projections $\mu^{\hat{X}}$ and $\mu^{\hat{S}}$, in the same manner as in eq. 2.28. The subspace projections with respect to $\mu^{\hat{S}}$ are solved perturbatively for the amplitudes in the $\hat{S}$ operator, and the amplitudes for $\hat{X}$ are determined without approximations.

With regard to excitations involving only active orbitals, those excitations are classified as internal (I), and these are included in $\hat{X}$. Excitations involving both active and inactive orbitals are classified as semi-external (SE), and the excitations involving only inactive orbitals are classified as external (E). Both the semi-external and external excitations are included in $\hat{S}$ [25, 30]. An advantage here would be to completely take advantage of the fact that the electron correlation is a local property by combining MLCC with localized orbitals, which would result in a reduction in computational scaling and computational cost, making the calculations more efficient.

### 2.5.3 Theoretical speedup

The most demanding terms in full CC3 scale as $V^4O^3$, where V is the number of virtual orbitals and O is the number of occupied orbitals in a full computation [15]. And this is reduced to $VV_A^3O_A^3$ in MLCC3, where $V_A$ is the number of active virtual orbitals and $O_A$ is the number of active occupied orbitals. Furthermore the theoretical speedup factor is given by

$$\eta_{theo} = \Big(\frac{V \times O}{V_A \times O_A}\Big)^3 \tag{2.38}$$

In practice, a CCSD/CC3 calculation will rarely come close to the theoretical speedup factor because the CCSD calculation scales as $V^3O^3$ and usually dominates the calculations. And $\eta_{theo}$ are usually on the same level as the contribution from the $\Omega$ vector [15], but in practice there are other factors that would also dominate the calculation such as for example integral transformation [25], making the calculations slower than what the theoretical speedup would suggest [15]. The $\Omega$ vectors refers to the amplitude equations in the MLCC3 model, defined

as [25]:

$$\Omega_{\mu 1} = \langle \mu_1 | \exp(-X_2) \hat{H} \exp(X_2) | HF \rangle + \langle \mu_1 | [H, T_3] | HF \rangle = \Omega_1^{CCSD} + \langle \mu_1 | [H, T_3] | HF \rangle = 0 \tag{2.39}$$

$$\Omega_{\mu 2} = \langle \mu_2 | \exp(-X_2) \hat{H} \exp(X_2) | HF \rangle + \langle \mu_2 | [H, T_3] | HF \rangle = \Omega_2^{CCSD} + \langle \mu_2 | [H, T_3] | HF \rangle = 0 \tag{2.40}$$

$$\Omega_{\mu_3^T} = \langle \mu_3^T | [\hat{H}, T_3] + [\hat{H}, X_2] + [[\hat{H}, X_2], X_2] + [[\hat{H}, T_3], X_2] | HF \rangle = 0 \tag{2.41}$$

### 2.5.4 Correlated natural transition orbitals for MLCC models

Høyvik, Myhre and Koch [15] have presented a procedure for obtaining an automatic selection of the active space in multilevel CC calculations. The procedure for generating these orbitals which is called Correlated natural transition orbitals (CNTOs), is a black box procedure for determining the active space where the high level treatment is carried out. The eigenvalues of the diagonalization provides hierarchical route for which orbitals are to be included in the orbital space. This results in the possibility of, rather than preselecting an active region of the molecule, a threshold is used for which eigenvalues with corresponding orbitals to be inlcuded. In the limit where the threshold is zero, the full orbital space is included in the active space and the entire molecular system is treated with high level theory.

The excitation energies, in CC response theory, are usually determined as the eigenvalues of the non-symmetric CC Jacobian. For example for excitation $\omega$, we have

$$\mathbf{AR} = \omega \mathbf{R} \tag{2.42}$$

where the CC Jacobian is defined as

$$A_{\mu\nu} = \frac{\partial \Omega_\mu}{\partial t_\nu} \tag{2.43}$$

The right excitation vector $\mathbf{R}$ of equation 2.42 contains single and double excitation components $\mathbf{R}_1$ and $\mathbf{R}_2$.

Then by using the excitation vector of equation 2.42 orthogonal transformation matrices for the occupied and virtual orbitals may be generated which gives the CNTOs. The CNTOs are obtained by constructing and diagonalizing an occupied-occupied matrix, $\mathbf{M}$, and a virtual-virtual matrix, $\mathbf{N}$, from the excitation vectors.

$$M_{ij} = \sum_a R_{ai} R_{aj} + \frac{1}{2} \sum_{abk} (1 + \delta_{ai,bk}\delta_{ij}) R_{aibk} R_{ajbk} \tag{2.44}$$

$$N_{ab} = \sum_i R_{ai} R_{bi} + \frac{1}{2} \sum_{ijc} (1 + \delta_{ai,cj}\delta_{ab}) R_{aicj} R_{bicj} \tag{2.45}$$

Then the matrices $\mathbf{M}$ and $\mathbf{N}$ are diagonalized as

$$\mathbf{M}u_i = \lambda_i^o u_i, \qquad i = 1, ..., n_{occ} \tag{2.46}$$

$$\mathbf{N}v_a = \lambda_a^v v_a, \qquad a = 1, ..., n_{vir} \tag{2.47}$$

Furthermore the normalization of the excitation vector gives

$$\sum_{ai} R_{ai}R_{ai} + \frac{1}{2}\sum_{aibj}(1+\delta_{ai,bj})R_{aibj}R_{aibj} = 1 \tag{2.48}$$

Such that $Tr(M) = Tr(N) = 1$ and $\sum_i \lambda_i^o = 1.0$ and $\sum_a \lambda_a^v = 1.0$. The eigenvectors of **M** and **N** make up the transformation matrices for the occupied and virtual space that generate the CNTOs. With respect to which CNTOs to include in the active space of the MLCC calculation, the sum of the eigenvalues is used. Ordering the orbitals with descending $\lambda_i^o$ and $\lambda_a^v$ to be included in the active space within given thresholds $\delta_o$ and $\delta_v$.

$$1 - \sum_{i \in act} \lambda_i^o < \delta_o \tag{2.49}$$

$$1 - \sum_{a \in act} \lambda_a^v < \delta_v \tag{2.50}$$

This thesis project will undertake an investigation of the preformance of the CNTOs in MLCC computation of valence excitations.

## 2.6 Basis sets

One way of approximation involving almost all ab initio calculation methods is the use of basis sets. Although it will not be an approximation if the basis set is a complete basis set, because a complete set consist of an infinite number of basis functions, but that is impossible to achive in practice. So in practice a finite basis set is used. It is common to represent a molecular orbital (MO) as a function in an infinite coordinate system that is spanned by a complete basis. And with respect to a finite basis set, then the only components of the MO that is represented are those along the axis.

There are two types of basis functions that are most commenly used in ab initio calculations, Slater type orbitals (STOs) and Gaussian type orbitals (GTOs) [35]. The STOs have

no radial nodes, radial nodes only occur when linear combinations of STOs are created. An advantage is that they converge fast because of their exponential dependency. The disadvantage regarding STOs is that they cannot be used for calculations on three and four centered or more centered two electron integrals. Because of this they are most often used on atomic or diatomic systems where high accuracy is desired. GTOs have a $r^2$ dependence in the exponent which gives two disadvantages. Problem one is they have a zero slope at the nucleus, where the STOs have a cusp, resulting in a problematic representation of proper behavior near the nucleus. Problem two is the GTOs fall off too rapidly far from the nucleus resulting in a poor representation of the tail. Because of these disadvantages with the GTOs are the reason that more of them are needed to achieve the same level of accuracy as the STOs. However, even if more GTOs are needed to achieve the same level of accuracy, their integrals are fairly easy to compute, and because of that the GTOs are the preferred basis functions in electronic structure calculations [35].

### 2.6.1 Basis set Classification

A minimal basis set contains just enough functions required to describe all the electrons of neutral atoms, meaning one basis function is used to describe each atomic orbital [35]. Basis sets can further be improved, where for example the basis functions can be doubled creating a Double Zeta (DZ) type basis. And for a Triple Zeta basis set, the number of basis functions are tripled and so on. Another possibility is to double the valence functions and keep the core functions minimal, creating a split valence basis set. Higher angular momentum is needed if electron correlation methods are being used. As stated in Section 2.3, there are two types of electron correlation. The basis set needs functions of the same type and different exponents to describe radial correlation. But the basis set needs functions with exponents of the same magnitude for different angular momentum, to describe angular correlation.

### 2.6.2 Correlation consistent basis sets

The purpose of correlation consistent (cc) basis sets, developed by Dunning et al. [18], is to describe the correlation energy of the valance electrons. These basis sets are known as cc-pVXZ ($X = D, T, Q, 5, ..$), for a polarized X-Zeta Gaussian basis set. The basis set can be optimized further with one extra function that has a smaller exponent for each angular momentum. And finally it is possible to add functions with large exponents, known as tight functions, if the purpose is to recover the core-core and core-valence correlation energy, and the acronym will then be cc-CVXZ ($X = D, T, Q, 5, ..$) [18, 35]. Since this thesis will focus on valence excitation energies, then the basis sets that will be used in this thesis are aug-cc-pVXZ ($X = D, T, Q, 5, ..$), where augmented functions have been added to the basis sets cc-pVXZ. Augmented functions are diffuse functions, who's purpose is to improve the flexibility in the outer valence region. Specifically in this thesis, the basis set that will be used is aug-cc-pVDZ, when calculating the valence excitation energies.

# Chapter 3

# Molecules

In this section, a short introduction about each molecule will be presented. In this thesis is a study involving four explosive molecules, NTO, fox-7, butanal which is an ordinary organic molecule and 4-nitroaniline which is also an organic molecule involving charge transfer (CT) excitation energies.

## 3.1 NTO

3-Nitro-1,2,4-triazole-5-one (NTO), as shown in figure 2.1, was developed at Los Alamos National Laboratory in 1983, and was found to have desireable characteristics such as high energy release on docomposition, high detonation velocity and good thermal stability etc. It has been characterized as a potential candidate for high energy density material (HEDM) which is powerful and yet resistant to accidental and sympathetic initiation. NTO has a lower shock sensitivity than TNT, and just as high explosive performance as RDX and HMX, which are the most effective and widely used explosives today. NTO is unique among military explosives in that it does not fall in traditional classes of explosives i.e. nitrates, nitramine or nitroaromatics. NTO is acidic and could coordinate with metallic ions. Another intresting feature of NTO is that there exist a possibility for inter or intra molecular hydrogen bonding [36].

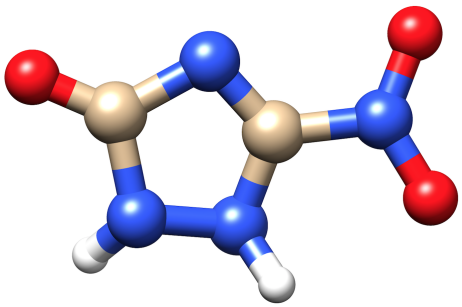

Figure 3.1: NTO

## 3.2 Fox-7

Fox-7 (1,1-diamino-2,2-dinitroethylene, $C_2H_4N_4O_4$) has recently been an attractive molecule for research into developing new energetic materials and explosives. Fox-7 is described as a push-pull molecule with two electron donor amine groups ($-NH_2$) and two electron withdrawing nitro groups ($-NO_2$) as shown in figure 2.4. It's insensitivity behaviour can be explained by it's structure, where Fox-7 is stable partially due to the strong intra-molecular hydrogen bonds between the nitro oxygen atoms and the amino hydrogen atoms, which is important for its ground and excited state properties. Furthermore compared to the presently most widely used and powerful explosives RDX and HMX, Fox-7 yields the same number of moles (0.0405) of gaseous product per gram of compound for the complete decomposition reaction to $CO_2$, $N_2$, and $H_2O$ [37].

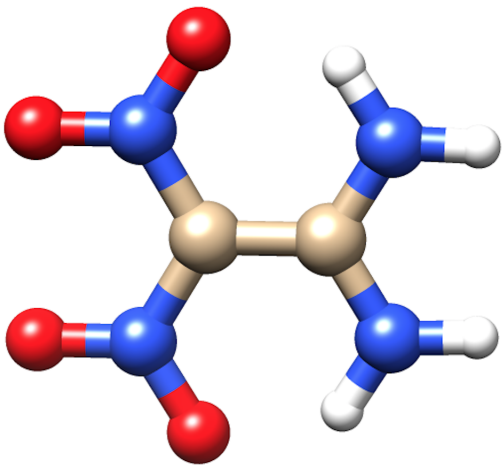

Figure 3.2: Fox-7

## 3.3 Butanal

Butanal is an organic compound with molecular formula $C_4H_8O$. It is an aldehyde derivative of Butane as shown in figure 2.6. It is flammable, colorless with acrid smell, mostly used as an organic solvent.

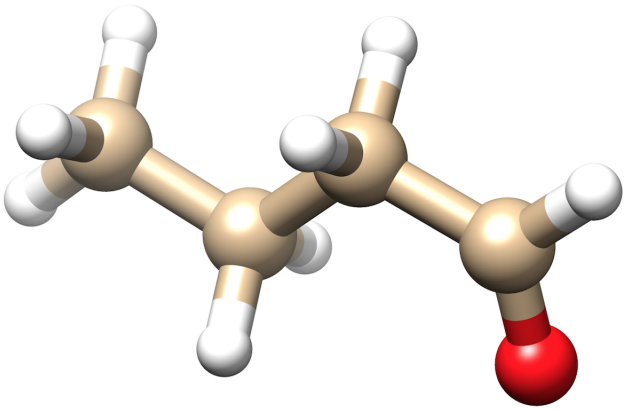

Figure 3.3: Butanal

## 3.4 4-Nitroaniline

4-Nitroaniline is composed of a benzene ring with a nitro group and an amino group bonded to its benzene ring. It is a synthetic precursor to Pharmaceuticals, dyes and pesticides and is a common wastewater contaminant. In high concentrations it can have a detrimental environmental effect as it is a carcinogen [16, 22].

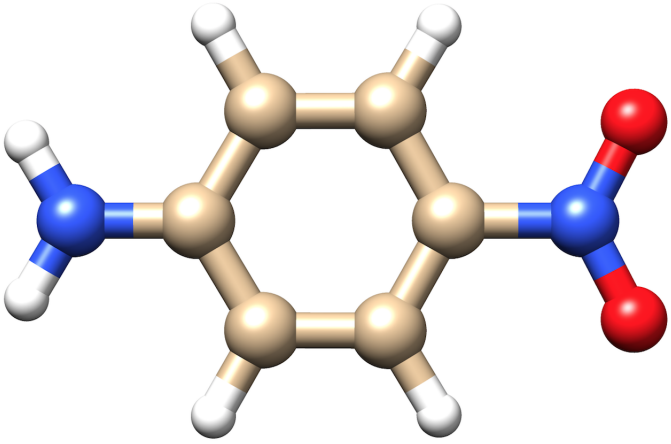

Figure 3.4: 4-Nitroaniline

# Chapter 4

# Results and discussion

In this section, a description of the procedure used for investigating valence excitation energies for a set of thresholds for CNTOs using the MLCC3 model on six different molecules, and the full CC3 model as a reference on four of the molecules. The results presented in table 4.1-4.4 will be evaluated in terms of the average errors per molecule and the average errors per excitation, and further compared with the percentage of active orbitals and the theoretical speedup factors.

## 4.1 Computational details

The geometry of the molecules; Butanal, NTO, Fox-7 and 4-nitroaniline [1–4] were optimized using the MP2 model with the cc-pVDZ basis set. The geometry optimizations were preformed using the qchem 4.4 program [5, 33] and the valence excitation energies were preformed with a local version of the DALTON program package [6]. The valence excitation energies were calculated using with the CCSD, MLCC3 and CC3 methods for the four smallest molecules; Butanal, NTO, Fox-7 and 4-nitroaniline. And for the two largest molecules the energies were calculated using only the CCSD and MLCC3 method, because they were too large for CC3.

For the excitation energies calculated with the MLCC3 model, they were calculated for a set of thresholds for $\delta_o$ and $\delta_v$, in the ranges of $10^{-3}$ to $10^{-4}$ for $\delta_o$ and $10^{-3}$ to $10^{-5}$ for $\delta_v$. The basis set aug-cc-pVDZ was used on all four molecules for calculations involving valence excitation energies. The valence excitation energies obtained using CNTOs and the MLCC3 model is presented in tables 4.1 - 4.4.

Tables 4.1 - 4.4 contain the results for NTO, fox-7, butanal, 4-nitroaniline. $\Delta(eV)$ in table 4.1 - 4.4 is the average error in eV computed according to the formula

$$\Delta(eV) = \frac{1}{5}\sum_{i=1}^{5} |exc(i) - CC3(i)| \tag{4.1}$$

where $exc(i)$ is the energy in eV for excitation i within a corresponding threshold, and CC3(i) is the CC3 energy of excitation i in eV.

The errors in each table denoted err.i, is the difference between the excitation energy for excitation i (exc.i) and the CC3(i) energy, where $i = 1, 2, 3, 4, 5$, within a corresponding threshold. And the values specified in parentheses, are the error in precentage with respect to the CCSD-CC3 difference.

## 4.2 The effects of $\delta_o$ and $\delta_v$

### 4.2.1 Considering average errors per molecule

For all of these molecules we have computed the five lowest valence excitation energies. Figure 4.1 shows the average errors per molecule relative to the CCSD-CC3 difference in precentage (%).

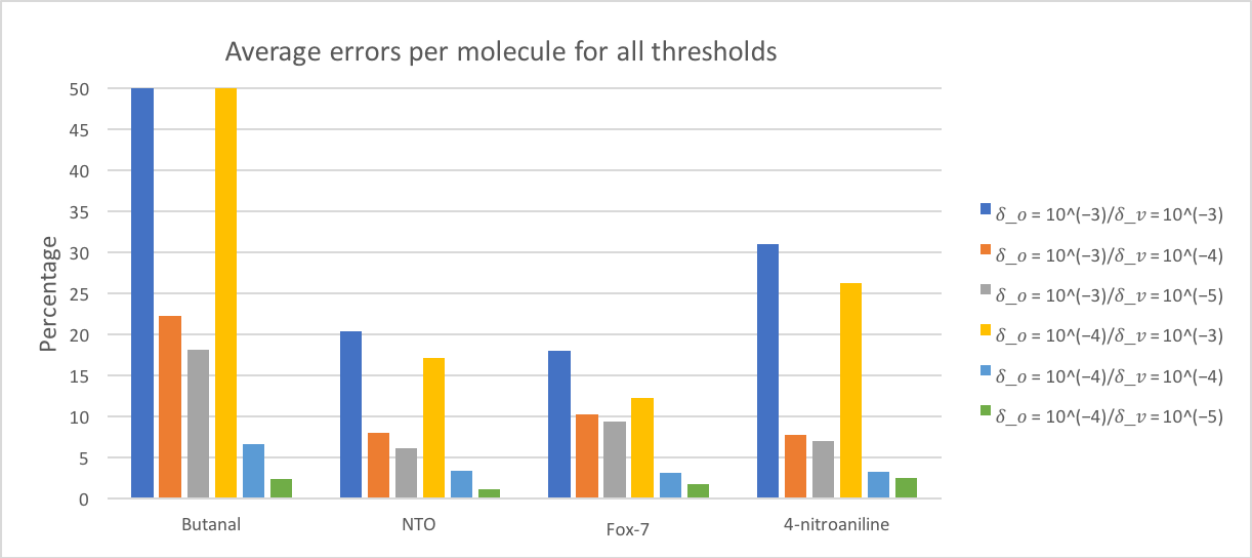


Figure 4.1: Average errors per molecule for every thresholds relative to the CCSD-CC3 difference, the $\delta_o = 10^{-3}/\delta_v = 10^{-3}$ for butanal goes up to 99% and the $\delta_o = 10^{-4}/\delta_v = 10^{-3}$ threshold goes up to 86% for butanal.

Considering the results from figure 4.1, we see that both combinations of thresholds containing $\delta_v = 10^{-3}$ give errors with far too high percentage compared to the CCSD-CC3 difference. We see in figure 4.1 that the results for butanal shows an average error of 99% for the $\delta_o = 10^{-3}/\delta_v = 10^{-3}$ threshold and 86% for the $\delta_o = 10^{-4}/\delta_v = 10^{-3}$ threshold. These are significantly large errors compared to the other molecules. There is no good explanation as to why this has occured, and also taking into account that figure 4.2 does not show any significantly less amount of active orbitals.

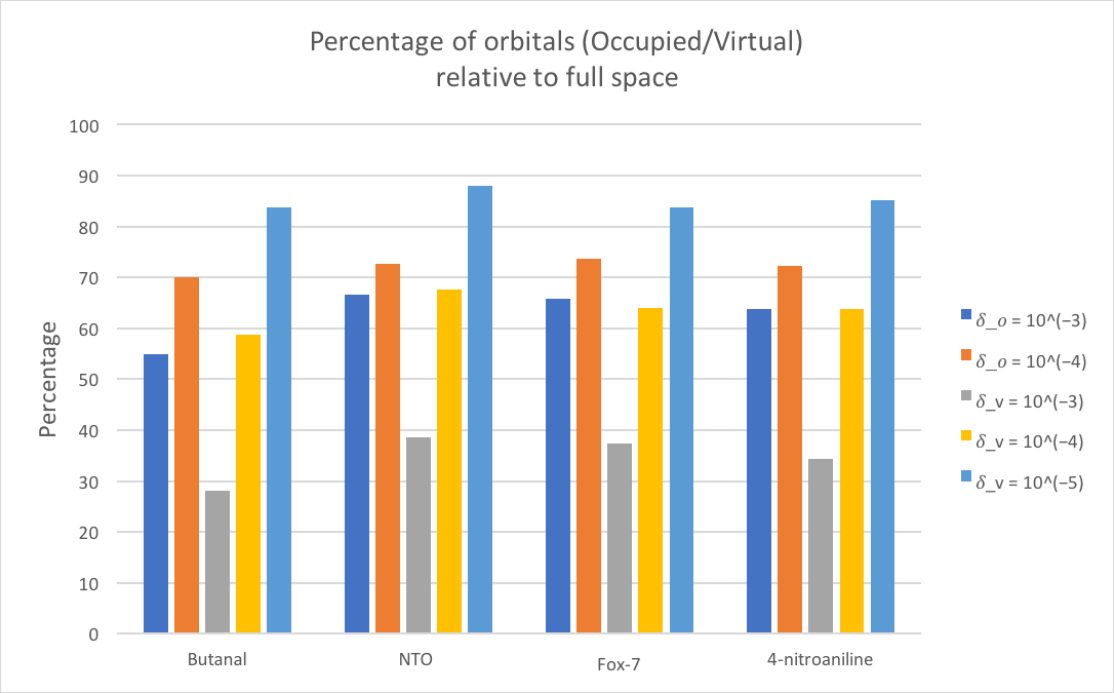


Figure 4.2: Percentage of active orbitals relative to full space

From figure 4.2 we see that generally the same percentage of orbitals are inlcuded in the active space for NTO, fox-7 and 4-nitroaniline for every threshold. But a little smaller percentage of orbitals are included in the active space for butanal for every thresholds. But this does not explain the significantly large errors observed for butanal. Parhaps some systematic errors occurred when running the calculations for butanal, for example that the system read a wrong file, or that the information in a file is wrong. However we refer to "future work " in chapter 5, with respect to the calculations concerning butanal, where we suggest these calculations be done again and double checked.

Furthermore by looking at table 4.1 we see that excitation number 2 and 4 for butanal has errors over 100% compared to the CCSD-CC3 difference for the $\delta_o = 10^{-3}/\delta_v = 10^{-3}$ threshold, which should never happen. We should normally see an improvement in accuracy as we increase the level of theory, and not a decline in accuracy. We can however conclude that $\delta_v = 10^{-3}$ is generally too high for the virtual space. And because of the fact that

$\delta_v = 10^{-3}$ gives such poor results generally, we will exclude $\delta_v = 10^{-3}$ from further discussions of our results, and have presented the same figures of average errors per molecule in figure 4.3 without the $\delta_v = 10^{-3}$ thresholds.

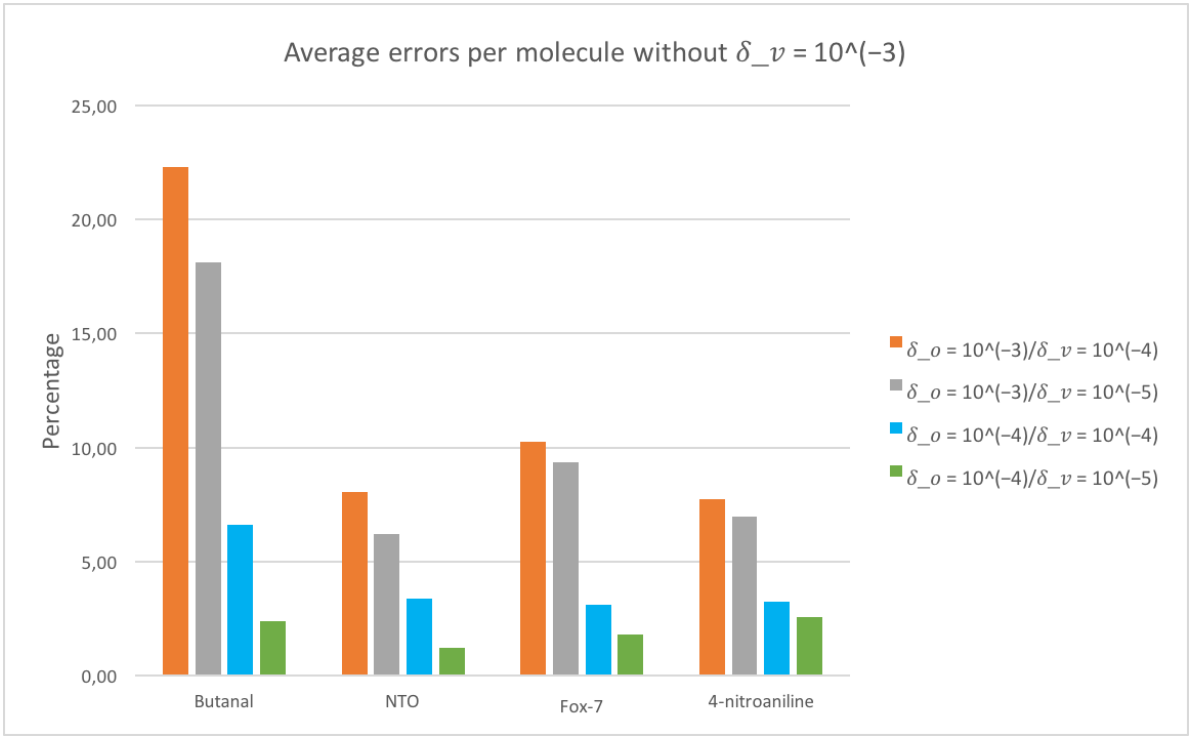


Figure 4.3: Average errors per molecule for every thresholds in percentage (%), except thresholds containing $\delta_v = 10^{-3}$.

Considering the results from figure 4.3, we see again that butanal has large errors for thresholds containing $\delta_o = 10^{-3}$ compared to the other molecules, where the $\delta_o = 10^{-3}/\delta_v = 10^{-4}$ gives 22.3% average error and $\delta_o = 10^{-3}/\delta_v = 10^{-5}$ gives 18.1% average error for butanal. A reason for this can be that for these thresholds containing $\delta_o = 10^{-3}$ give somewhat less amount of active orbitals for butanal than the other molecules as shown by figure 4.2. We can then conclude that $\delta_o = 10^{-3}$ is too high for the occupied space for butanal. However we observe a significant improvement in the errors for butanal as we tighten the threshold for the occupied space from $\delta_o = 10^{-3}$ to $\delta_o = 10^{-4}$. For NTO, fox-7 and 4-nitroaniline we observe good results for all the thresholds $\delta_o = 10^{-3}/\delta_v = 10^{-4}$, $\delta_o = 10^{-3}/\delta_v = 10^{-5}$, $\delta_o = 10^{-4}/\delta_v = 10^{-4}$ and $\delta_o = 10^{-4}/\delta_v = 10^{-5}$, where they give an average error in the

ranges from 1.2% for $\delta_o = 10^{-4}/\delta_v = 10^{-5}$ for NTO to 10.3% for $\delta_o = 10^{-3}/\delta_v = 10^{-4}$ for fox-7.

The results in figure 4.3 show an increase in accuracy as we tighten the thresholds from $\delta_o = 10^{-3}/\delta_v = 10^{-4}$ to $\delta_o = 10^{-4}/\delta_v = 10^{-5}$. This is to be excpected as we also increase the precentage of active orbitals from from $\delta_o = 10^{-3}/\delta_v = 10^{-4}$ to $\delta_o = 10^{-4}/\delta_v = 10^{-5}$ as shown in figure 4.2, especially for the occupied space which increases from 55% to 70% for the active occupied orbitals for butanal.

With respect to butanal, we have to tighten the threshold to $\delta_o = 10^{-4}/\delta_v = 10^{-5}$ in order to get an average error in the same precentage level as NTO, fox-7 and 4-nitroaniline. Where $\delta_o = 10^{-4}/\delta_v = 10^{-5}$ gives an average error of 2.4% for butanal, 1.2% for NTO, 1.8% for fox-7 and 2.6 % for 4-nitroaniline.

On the other hand $\delta_o = 10^{-4}/\delta_v = 10^{-4}$ gives an average error for NTO, fox-7 and 4-nitroaniline on approximately the same level of percentage. Where the average error is 3.4% for NTO, 3.1% for fox-7 and 3.3% for 4-nitroaniline. The figure 4.3 shows that the average error for butanal deviates from this percentage level, where butanal shows an average error of 6.4% for $\delta_o = 10^{-4}/\delta_v = 10^{-4}$, which is approximately double the value of error compared to the values for NTO, fox-7 and 4-nitroaniline.

The same observation is seen with respect to butanal for the thresholds $\delta_o = 10^{-3}/\delta_v = 10^{-4}$ and $\delta_o = 10^{-3}/\delta_v = 10^{-5}$, where butanal shows approximately either double or triple the value of average error compared to NTO, fox-7 and 4-nitroaniline. And when we also consider the high theoretical speedup factor equal to 30 for $\delta_o = 10^{-3}/\delta_v = 10^{-4}$ for butanal in figure 4.4, indicates the result for $\delta_o = 10^{-3}/\delta_v = 10^{-4}$ for butanal is too unreliable and inaccurate in order to for example be able to support experimentalists.

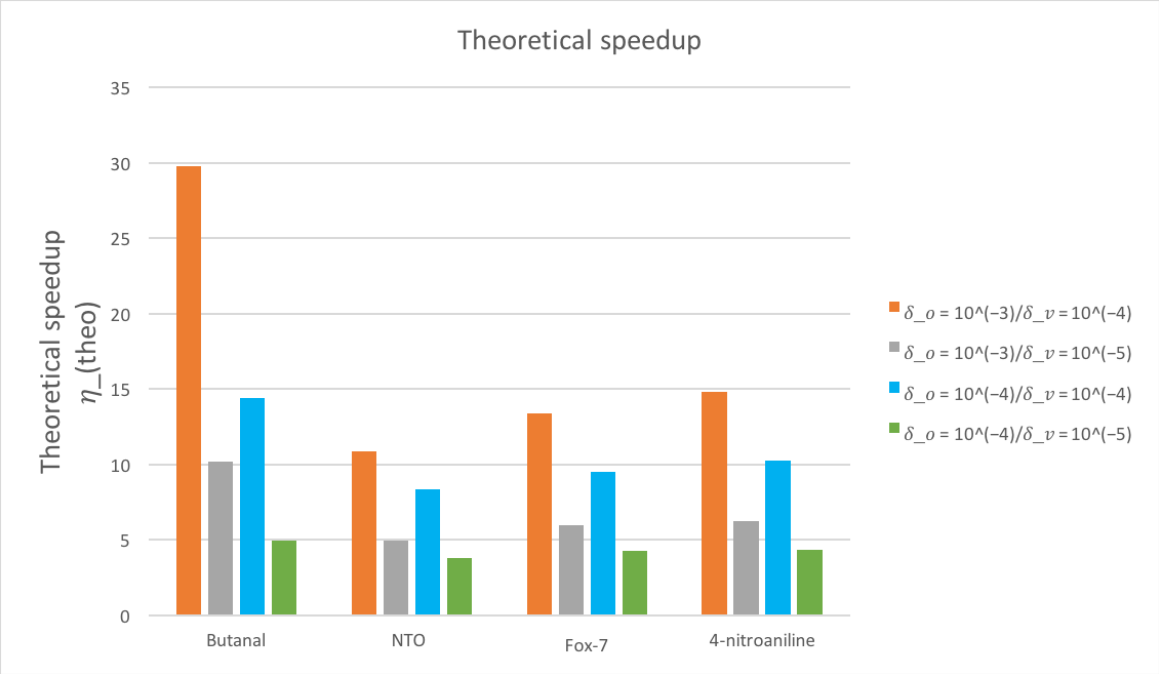


Figure 4.4: Theoretical speedup for thresholds without $\delta_v = 10^{-3}$ for NTO, fox-7, butanal and 4-nitroaniline

Also by comparing the average errors for the thresholds $\delta_o = 10^{-3}/\delta_v = 10^{-5}$ and $\delta_o = 10^{-4}/\delta_v = 10^{-4}$ for butanal, we see that $\delta_o = 10^{-3}/\delta_v = 10^{-5}$ gives an average error of 18.1% with a theoretical speedup factor equal to 10.2, and $\delta_o = 10^{-4}/\delta_v = 10^{-4}$ gives an average error of 6.6% with a theoretical speedup factor equal to 14.4. So $\delta_o = 10^{-4}/\delta_v = 10^{-4}$ gives a higher theoretical speedup factor with a lower average error compared to $\delta_o = 10^{-3}/\delta_v = 10^{-5}$ which gives a lower theoretical speedup with a higher average error. A reason for this would be the different percentage of active orbitals, especially for the occupied space. Where $\delta_o = 10^{-3}/\delta_v = 10^{-5}$ has 55% active occupied orbitals and 83.8% active virtual orbitals, compared to $\delta_o = 10^{-4}/\delta_v = 10^{-4}$ which gives 70% active occupied orbitals and 58.7% active virtual orbitals. This indicates that the level of accuracy in the average error is highly dependent on the active occupied space. And it also indicates that its more worth looking at $\delta_o = 10^{-4}/\delta_v = 10^{-4}$ threshold then the $\delta_o = 10^{-3}/\delta_v = 10^{-5}$ threshold. This observation can be seen generally in figure 4.3 for NTO, fox-7 and 4-nitroaniline, where we see a good

improvement in the average error when we go from $\delta_o = 10^{-3}$ to $\delta_o = 10^{-4}$.

As stated before we have to approach the $\delta_o = 10^{-4}/\delta_v = 10^{-5}$ threshold before we get average errors per molecule which are accurate, reliable and on the same level of percentage. Because for the other thresholds, the average errors varies more from molecule to molecule and from threshold to threshold. But for $\delta_o = 10^{-4}/\delta_v = 10^{-5}$ the average error is more consistent for each molecule. The theoretical speedup factor (figure 4.4) and the percentage of active orbitals (figure 4.2) are also consistently on the same level for each molecule.But this is not the case for the other thresholds. Which means there is no point in doing calculations with higher theoretical speedup, when the results varies from molecule to molecule and also giving inconsistent and inaccurate average errors, which means those result are too unreliable to for example support experimentalists.

### 4.2.2 Considering average errors per excitation

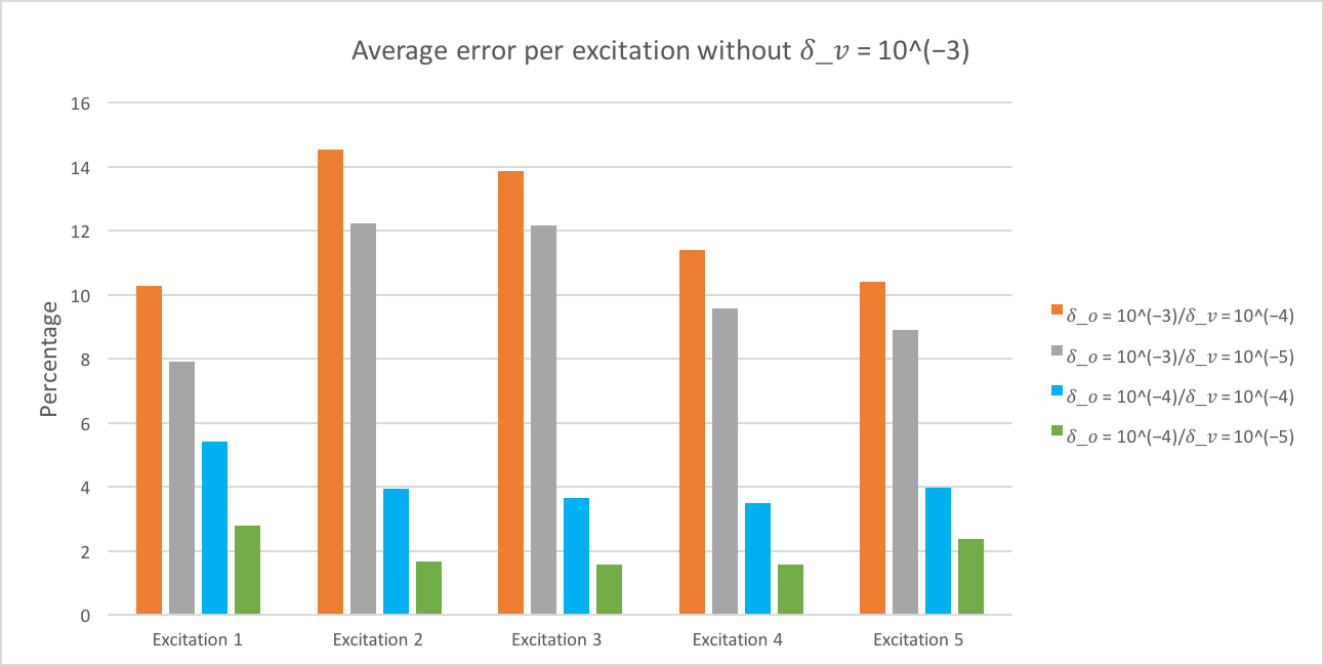


Figure 4.5: Average errors per excitation for every thresholds relative to the CCSD-CC3 difference in percentage (%), except for thresholds containing $\delta_v = 10^{-3}$.

Considering the results in figure 4.5, the same trend is observed for each excitation, where the results give more and more accurate errors, the tighter the thresholds become. And this is due to the obvious reason, where the tighter the threshold means a larger amount of the molecule is treated with higher level of theory so we would expect more and more accurate results. However for thresholds containing $\delta_o = 10^{-3}$, we see excitation number 1 has the smallest errors, and the errors increase for excitation 2, and then decrease steadily for excitation 3,4 and 5. But for thresholds containing $\delta_o = 10^{-4}$, we observe excitation 1 has the highest errors, and the average errors decrease steadily for exciation 2, 3 and 4, and then increase a little for excitation 5. This could be due to the higher excitations being more diffuse. However the errors are much larger for the $\delta_o = 10^{-3}$ thresholds compared to the $\delta_o = 10^{-4}$ thresholds, so we would consider using $\delta_o = 10^{-4}$ to obtain accurate results for the occupied space. We do not observe a significcant improvement in the average errors for the virtual space when we go from $\delta_v = 10^{-4}$ to $\delta_v = 10^{-5}$, but a reasonable improvement is

observed nonetheless. This is related to the higher amount of active orbitals included in the virtual space when we go from $\delta_v = 10^{-4}$ to $\delta_v = 10^{-5}$ as shown by figure 4.2.

We see from figure 4.5 that the average errors per exciation for the threshold $\delta_o = 10^{-3}/\delta_v = 10^{-4}$ are in the ranges from 10.3% for excitation number 1 to 14.5% for excitation number 2, where excitation 2 gives the highest percentage of average error for $\delta_o = 10^{-3}/\delta_v = 10^{-4}$. And for $\delta_o = 10^{-3}/\delta_v = 10^{-5}$ the average error ranges from 7.9% for excitation 1 to 12.2 % for excitation 2, where excitation 2 is the highest precentage of error for $\delta_o = 10^{-3}/\delta_v = 10^{-5}$. By considering the fact that from the previous section we observed that butanal have a high average error for these thresholds compared to NTO, fox-7 and 4-nitroaniline, and also by looking at table 4.1-4.4 we see that butanal generally shows higher percentage of errors compared to NTO, fox-7 and 4-nitronaniline. By that reasoning butanal gives a strong contribution to the average error per excitation, and NTO, fox-7 and 4-nitroaniline generally show percentage of errors approximately on the same level with respect to each other. Let us therefore look at a version of figure 4.5 without the contribution from butanal as shown in figure 4.6.

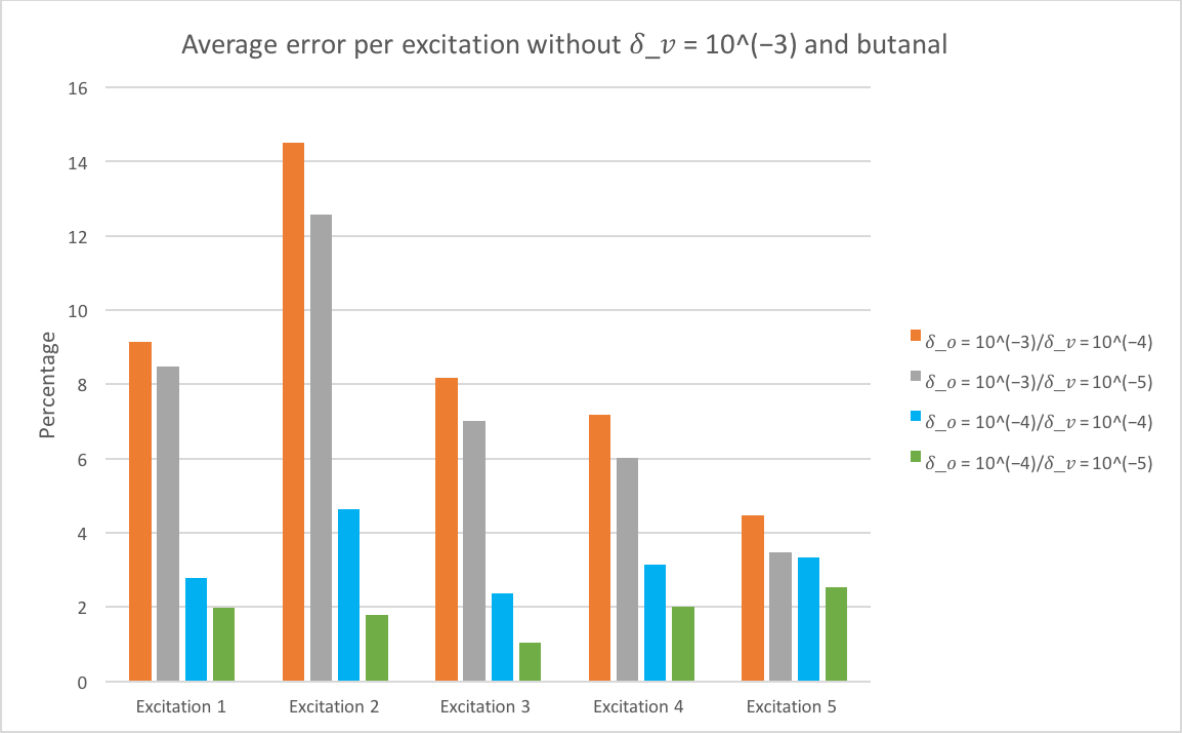


Figure 4.6: Average errors per excitation for every thresholds relative to the CCSD-CC3 difference in percentage (%), except for thresholds containing $\delta_v = 10^{-3}$ and the contribution from butanal.

We now observe a significant difference in the average error per excitation from figure 4.5 to figure 4.6. For the threshold $\delta_o = 10^{-3}/\delta_v = 10^{-4}$, we observe a general decrease in average error from 9.1% for excitation 1 to 4.5% for excitation 5, except for a deviation for excitation 2 which has an average error of 14.5% and is approximately unchanged from figure 4.5. The same trend is observed for the $\delta_o = 10^{-3}/\delta_v = 10^{-5}$ threshold in figure 4.6, where excitation 1 has an average error of 8.5% and it decreases to 3.5% for excitation 5, with the exception of excitation 2 which shows an average error of 12.5% and is approximately unchanged from figure 4.5. The reason that the average error is unchanged for excitation 2 for $\delta_o = 10^{-3}/\delta_v = 10^{-4}$ and $\delta_o = 10^{-3}/\delta_v = 10^{-5}$ is because NTO and fox-7 has a couple of high percentage errors for excitation 2, as seen from table 4.2 and table 4.3. However for the $\delta_o = 10^{-4}/\delta_v = 10^{-4}$ threshold, figure 4.5 shows that the average errors approaches a consistent level of percentage for excitation 2-5 in the ranges from 3.5%-3.9%, and a little

higher average error of 5.4% for excitation 1. Comparing figure 4.5 and figure 4.6 we can see that butanal is the one driving up the average error in figure 4.5 for excitation 1 for $\delta_o = 10^{-4}/\delta_v = 10^{-4}$. For the $\delta_o = 10^{-4}/\delta_v = 10^{-4}$ threshold in figure 4.6 the same trend can be observed where for excitation 1-5 are consistently on the same level of average errors in the ranges 2.4% -4.6%, and a little deviation for excitation 2 which shows an average error of 4.6 %. The reason for the little increase in error from figure 4.5 to figure 4.6 for excitation 2 is because NTO has a relatively high percentage error as shown in table 4.2.

As for the $\delta_o = 10^{-4}/\delta_v = 10^{-5}$ threshold, it shows consistent average errors approximately on the same level of percentage ranging from 1.5% - 2.78% for figure 4.5 and from 1.0%-2.5% for figure 4.6. We generally see a significant improvement in accuracy when going from the $\delta_o = 10^{-3}$ to $\delta_o = 10^{-4}$ for the occupied space, due to the increase in percentage of active orbitals as stated before. And as mentioned before the average error per excitation converge towards approximately the same level of percentage. This makes $\delta_o = 10^{-4}/\delta_v = 10^{-5}$ accurate and reliable, just like we observed in the previous section.

We also genereally observe a decrease in average error, when going from $\delta_v = 10^{-4}$ to $\delta_v = 10^{-5}$, this is because of the increase in active virtual orbitals as shown in figure 4.2. But we observe a much larger improvement when going from $\delta_o = 10^{-3}$ to $\delta_o = 10^{-4}$ for the occupied space. So the increase in active occupied orbitals seems to have the biggest impact on the average errors both for the average errors per molecule and for average errors per excitation.

We also observe that the theoretical speedup factor is around the same level for $\delta_o = 10^{-4}/\delta_v = 10^{-5}$ ranging between 3.8 for NTO to 4.9 for butanal, which results in average errors around the same level, making these results reliable. But for the higher theoretical speedup factors for the other thresholds, results in more inaccurate and inconsistent average errors making those results unreliable, and so we can conclude that $\delta_o = 10^{-4}/\delta_v = 10^{-5}$ is

an acceptable threshold.

Table 4.1: Five lowest MLCC3 valence energies for butanal using aug-cc-pVDZ. They are computed in a combined CNTO basis. All excitation energies and errors are in eV.

| $log(\delta_o)$ | $log(\delta_v)$ | exc.1 | exc.2 | exc.3 | exc.4 | exc.5 | nocc | nvirt | $\Delta(eV)$ | err.1 | err.2 | err.3 | err.4 | err.5 |
|---|---|---|---|---|---|---|---|---|---|---|---|---|---|---|
| -3 | -3 | 4.278 | 6.706 | 7.414 | 7.529 | 7.646 | 11 | 47 | 0.060 | 0.019 | 0.058 | 0.081 | 0.069 | 0.075 |
| | | | | | | | | | | (91.6) | (107.3) | (96.8) | (108.4) | (91.0) |
| -3 | -4 | 4.262 | 6.655 | 7.359 | 7.475 | 7.594 | 11 | 98 | 0.015 | 0.003 | 0.008 | 0.026 | 0.015 | 0.023 |
| | | | | | | | | | | (13.7) | (14.6) | (30.9) | (24.0) | (28.2) |
| -3 | -5 | 4.260 | 6.654 | 7.356 | 7.473 | 7.592 | 11 | 140 | 0.013 | 0.001 | 0.006 | 0.023 | 0.013 | 0.021 |
| | | | | | | | | | | (6.2) | (11.2) | (27.7) | (20.2) | (25.2) |
| -4 | -3 | 4.279 | 6.699 | 7.400 | 7.518 | 7.632 | 14 | 47 | 0.051 | 0.02 | 0.051 | 0.066 | 0.058 | 0.06 |
| | | | | | | | | | | (92.5) | (94.8) | (79.3) | (91.3) | (73.5) |
| -4 | -4 | 4.262 | 6.649 | 7.340 | 7.463 | 7.576 | 14 | 98 | 0.004 | 0.003 | 0.001 | 0.006 | 0.003 | 0.005 |
| | | | | | | | | | | (13.3) | (1.9) | (7.5) | (4.6) | (5.9) |
| -4 | -5 | 4.260 | 6.647 | 7.336 | 7.460 | 7.573 | 14 | 140 | 0.001 | 0.001 | 0.001 | 0.003 | 0.0002 | 0.002 |
| | | | | | | | | | | (5.2) | (1.3) | (3.2) | (0.3) | (1.9) |
| Full | CC3 | 4.259 | 6.648 | 7.333 | 7.460 | 7.571 | 20 | 167 | | | | | | |
| Full | CCSD | 4.280 | 6.702 | 7.417 | 7.523 | 7.653 | 20 | 167 | | | | | | |
| | CCSD-CC3 | 0.021 | 0.054 | 0.083 | 0.063 | 0.082 | | | | | | | | |

Table 4.2: Five lowest MLCC3 valence energies for NTO using aug-cc-pVDZ. They are computed in a combined CNTO basis. All excitation energies and errors are in eV.

| $log(\delta_o)$ | $log(\delta_v)$ | exc.1 | exc.2 | exc.3 | exc.4 | exc.5 | nocc | nvirt | $\Delta(eV)$ | err.1 | err.2 | err.3 | err.4 | err.5 |
|---|---|---|---|---|---|---|---|---|---|---|---|---|---|---|
| -3 | -3 | 3.871 | 4.168 | 4.244 | 4.761 | 5.546 | 22 | 74 | 0.054 | 0.009 | 0.068 | 0.047 | 0.088 | 0.056 |
| | | | | | | | | | | (13.5) | (29.0) | (17.7) | (23.9) | (18.0) |
| -3 | -4 | 3.864 | 4.134 | 4.215 | 4.703 | 5.511 | 22 | 130 | 0.021 | 0.003 | 0.034 | 0.018 | 0.03 | 0.022 |
| | | | | | | | | | | (4.0) | (14.5) | (6.6) | (8.2) | (7.0) |
| -3 | -5 | 3.863 | 4.125 | 4.211 | 4.697 | 5.507 | 22 | 169 | 0.017 | 0.002 | 0.025 | 0.014 | 0.024 | 0.018 |
| | | | | | | | | | | (2.9) | (10.8) | (5.2) | (6.5) | (5.7) |
| -4 | -3 | 3.869 | 4.159 | 4.235 | 4.746 | 5.534 | 24 | 74 | 0.045 | 0.008 | 0.059 | 0.038 | 0.073 | 0.045 |
| | | | | | | | | | | (11.9) | (25.2) | (14.2) | (19.9) | (14.3) |
| -4 | -4 | 3.863 | 4.116 | 4.203 | 4.684 | 5.498 | 24 | 130 | 0.009 | 0.001 | 0.016 | 0.006 | 0.011 | 0.009 |
| | | | | | | | | | | (1.9) | (6.8) | (2.4) | (3.0) | (2.8) |
| -4 | -5 | 3.862 | 4.103 | 4.199 | 4.677 | 5.495 | 24 | 169 | 0.003 | 0.001 | 0.004 | 0.003 | 0.004 | 0.005 |
| | | | | | | | | | | (0.8) | (1.6) | (1.0) | (1.0) | (1.7) |
| Full | CC3 | 3.861 | 4.100 | 4.197 | 4.673 | 5.489 | 33 | 192 | | | | | | |
| Full | CCSD | 3.930 | 4.335 | 4.465 | 5.039 | 5.803 | 33 | 192 | | | | | | |
| | CCSD-CC3 | 0.069 | 0.235 | 0.268 | 0.365 | 0.314 | | | | | | | | |

Table 4.3: Five lowest MLCC3 valence energies for Fox-7 using aug-cc-pVDZ. They are computed in a combined CNTO basis. All excitation energies and errors are in eV.

| $log(\delta_o)$ | $log(\delta_v)$ | exc.1 | exc.2 | exc.3 | exc.4 | exc.5 | nocc | nvirt | $\Delta(eV)$ | err.1 | err.2 | err.3 | err.4 | err.5 |
|---|---|---|---|---|---|---|---|---|---|---|---|---|---|---|
| -3 | -3 | 3.705 | 4.182 | 4.530 | 4.767 | 4.811 | 25 | 85 | 0.037 | 0.011 | 0.03 | 0.053 | 0.06 | 0.031 |
| | | | | | | | | | | (10.6) | (30.8) | (13.9) | (22.5) | (12.6) |
| -3 | -4 | 3.701 | 4.171 | 4.504 | 4.741 | 4.795 | 25 | 146 | 0.020 | 0.007 | 0.019 | 0.027 | 0.034 | 0.014 |
| | | | | | | | | | | (6.5) | (19.1) | (7.1) | (12.9) | (5.8) |
| -3 | -5 | 3.701 | 4.170 | 4.498 | 4.737 | 4.791 | 25 | 191 | 0.018 | 0.007 | 0.019 | 0.021 | 0.03 | 0.011 |
| | | | | | | | | | | (6.7) | (18.9) | (5.5) | (11.3) | (4.4) |
| -4 | -3 | 3.702 | 4.170 | 4.519 | 4.745 | 4.806 | 28 | 85 | 0.026 | 0.008 | 0.018 | 0.042 | 0.038 | 0.026 |
| | | | | | | | | | | (7.2) | (18.7) | (11.0) | (14.2) | (10.6) |
| -4 | -4 | 3.697 | 4.156 | 4.488 | 4.715 | 4.787 | 28 | 146 | 0.007 | 0.003 | 0.004 | 0.011 | 0.008 | 0.007 |
| | | | | | | | | | | (2.4) | (4.2) | (2.9) | (3.0) | (3.0) |
| -4 | -5 | 3.697 | 4.155 | 4.480 | 4.710 | 4.783 | 28 | 191 | 0.003 | 0.003 | 0.003 | 0.003 | 0.003 | 0.003 |
| | | | | | | | | | | (2.5) | (3.1) | (0.8) | (1.3) | (1.3) |
| Full | CC3 | 3.694 | 4.152 | 4.477 | 4.707 | 4.780 | 38 | 228 | | | | | | |
| Full | CCSD | 3.798 | 4.251 | 4.862 | 4.973 | 5.027 | 38 | 228 | | | | | | |
| | CCSD-CC3 | 0.104 | 0.099 | 0.385 | 0.266 | 0.247 | | | | | | | | |

Table 4.4: Five lowest MLCC3 valence energies for 4-Nitroaniline using aug-cc-pVDZ. They are computed in a combined CNTO basis. All excitation energies and errors are in eV.

| $log(\delta_o)$ | $log(\delta_v)$ | exc.1 | exc.2 | exc.3 | exc.4 | exc.5 | nocc | nvirt | $\Delta(eV)$ | err.1 | err.2 | err.3 | err.4 | err.5 |
|---|---|---|---|---|---|---|---|---|---|---|---|---|---|---|
| -3 | -3 | 4.021 | 4.341 | 4.500 | 5.024 | 5.815 | 23 | 85 | 0.045 | 0.029 | 0.066 | 0.027 | 0.052 | 0.051 |
| | | | | | | | | | | (25.9) | (21.8) | (17.8) | (44.0) | (45.9) |
| -3 | -4 | 4.011 | 4.305 | 4.490 | 4.972 | 5.763 | 23 | 158 | 0.013 | 0.019 | 0.03 | 0.016 | 0.001 | 0.001 |
| | | | | | | | | | | (17.0) | (9.9) | (10.8) | (0.5) | (0.6) |
| -3 | -5 | 4.009 | 4.299 | 4.489 | 4.972 | 5.763 | 23 | 211 | 0.012 | 0.018 | 0.024 | 0.016 | 0.0004 | 0.0005 |
| | | | | | | | | | | (15.9) | (8.0) | (10.3) | (0.3) | (0.4) |
| -4 | -3 | 4.008 | 4.326 | 4.489 | 5.024 | 5.814 | 26 | 85 | 0.037 | 0.017 | 0.051 | 0.015 | 0.051 | 0.051 |
| | | | | | | | | | | (15.1) | (16.9) | (10.1) | (43.8) | (45.6) |
| -4 | -4 | 3.996 | 4.283 | 4.476 | 4.969 | 5.759 | 26 | 158 | 0.005 | 0.005 | 0.009 | 0.003 | 0.004 | 0.005 |
| | | | | | | | | | | (4.0) | (2.9) | (1.8) | (3.4) | (4.2) |
| -4 | -5 | 3.994 | 4.277 | 4.475 | 4.968 | 5.758 | 26 | 211 | 0.003 | 0.003 | 0.002 | 0.002 | 0.004 | 0.005 |
| | | | | | | | | | | (2.6) | (0.7) | (1.3) | (3.7) | (4.6) |
| Full | CC3 | 3.991 | 4.275 | 4.473 | 4.973 | 5.764 | 36 | 248 | | | | | | |
| Full | CCSD | 4.104 | 4.578 | 4.625 | 5.090 | 5.875 | 36 | 248 | | | | | | |
| | CCSD-CC3 | 0.112 | 0.303 | 0.151 | 0.117 | 0.111 | | | | | | | | |

# Chapter 5

# Conclusion

In this thesis project, valence excitation energies in the multilevel coupled cluster (CC3/CCSD) framework using correlated natural transition orbitals have been computed, and compared to valence excitation energies calculated with the full CC3 model. The correlated natural transition orbitals are included in an active space using a threshold for the eigenvalues corresponding to the orbitals. The calculated valence excitation energies from the MLCC3 model give both high and small errors compared to the full CC3 model. For example the $\delta_o = 10^{-3}/\delta_v = 10^{-3}$ and $\delta_o = 10^{-3}/\delta_v = 10^{-3}$ thresholds give high average errors per molecule of respectively 99% and 86% for butanal, 20% and 17% for NTO, 18% and 12% for fox-7, and finally 31% and 26% for 4-nitroaniline. However using $10^{-4}$ as a threshold for the active occupied orbitals and $10^{-5}$ as a threshold for the active virtual orbitals give accurate results of, 1.2%-2.6% for average error per molecule and 1.5%-2.8% in terms of average error per excitation, for the molecules used in this project. These accurate results are to be expected considering, between 70% and 74% of the occupied orbitals and between 83%-88% of the virtual orbitals are included in the active space. Which means a large percentage of the molecule is included in the active space for the $\delta_o = 10^{-4}/\delta_v = 10^{-5}$ threshold. In general to obtain errors less than 10% on needs to include approximately 60-70% of the orbital space for the investigated molecules. Clearly the correlated natural transition orbitals are appropriately adapted for electron transition in the valence region.

# Chapter 6

# Future work

The calculations for butanal resulted in significantly large errors as shown by figure 4.1, especially for thresholds containing $\delta_v = 10^{-3}$. There might have been some problems that occured when running these calculations, for example that the program accidentally have read a wrong file or a file contained wrong information. However these calculations should be done again and double checked to confirm that these are the right or wrong energies.

Valence excitation energy calculations using the MLCC3 framwork for the molecules RDX and TNT are still running, and these are to be included in the dataset when finished. Further, it could be of interest to investigate the use of CNTOs for charge-transfer excitations.

# References


[1] Butanal, 2017. URL https://pubchem.ncbi.nlm.nih.gov/compound/261.

[2] Nto, 2017. URL https://pubchem.ncbi.nlm.nih.gov/compound/3453883#section=Top.

[3] Fox-7, 2017. URL https://pubchem.ncbi.nlm.nih.gov/compound/536770.

[4] 4-nitroaniline, 2017. URL https://pubchem.ncbi.nlm.nih.gov/compound/7475.

[5] Q-chem, 2017. URL http://www.q-chem.com.

[6] K. Aidas, C. Angeli, K. L. Bak, V. Bakken, R. Bast, L. Boman, O. Christiansen, R. Cimiraglia, S. Coriani, P. Dahle, E. K. Dalskov, U. Ekström, T. Enevoldsen, J. J. Eriksen, P. Ettenhuber, B. Fernández, L. Ferrighi, H. Fliegl, L. Frediani, K. Hald, A. Halkier, C. Hättig, H. Heiberg, T. Helgaker, A. C. Hennum, H. Hettema, E. Hjertenæs, S. Høst, I.-M. Høyvik, M. F. Iozzi, B. Jansík, H. J. A. Jensen, D. Jonsson, P. Jørgensen, J. Kauczor, S. Kirpekar, T. Kjærgaard, W. Klopper, S. Knecht, R. Kobayashi, H. Koch, J. Kongsted, A. Krapp, K. Kristensen, A. Ligabue, O. B. Lutnæs, J. I. Melo, K. V. Mikkelsen, R. H. Myhre, C. Neiss, C. B. Nielsen, P. Norman, J. Olsen, J. M. H. Olsen, A. Osted, M. J. Packer, F. Pawlowski, T. B. Pedersen, P. F. Provasi, S. Reine, Z. Rinkevicius, T. A. Ruden, K. Ruud, V. V. Rybkin, P. Sałek, C. C. M. Samson, A. S. de Merás, T. Saue, S. P. A. Sauer, B. Schimmelpfennig, K. Sneskov, A. H. Steindal, K. O. Sylvester-Hvid, P. R. Taylor, A. M. Teale, E. I. Tellgren, D. P. Tew, A. J. Thorvaldsen, L. Thøgersen, O. Vahtras,

M. A. Watson, D. J. D. Wilson, M. Ziolkowski, and H. Ågren. The dalton quantum chemistry program system. *Wiley Interdisciplinary Reviews: Computational Molecular Science*, 4(3):269–284, 2014. ISSN 1759-0884. doi: 10.1002/wcms.1172. URL `http://dx.doi.org/10.1002/wcms.1172`.

[7] P. Atkins and R. Friedman. *Molecular Quantum Mechanics*, volume 5. edition. OUP Oxford, 2011.

[8] P. Baudin and K. Kristensen. Lofex — a local framework for calculating excitation energies: Illustrations using ri-cc2 linear response theory. *The Journal of Chemical Physics*, 144(22):224106, 2016. doi: 10.1063/1.4953360. URL `http://dx.doi.org/10.1063/1.4953360`.

[9] J. L. Bentz, R. M. Olson, M. S. Gordon, M. W. Schmidt, and R. A. Kendall. Coupled cluster algorithms for networks of shared memory parallel processors. *Computer Physics Communications*, 176(9–10):589 – 600, 2007.

[10] O. Christiansen, H. Koch, and P. Jo/rgensen. Response functions in the cc3 iterative triple excitation model. *The Journal of Chemical Physics*, 103(17):7429–7441, 1995.

[11] O. Christiansen, P. Manninen, P. Jørgensen, and J. Olsen. Coupled-cluster theory in a projected atomic orbital basis. *The Journal of Chemical Physics*, 124(8):084103, 2006.

[12] S. Coriani and H. Koch. Communication: X-ray absorption spectra and core-ionization potentials within a core-valence separated coupled cluster framework. *The Journal of Chemical Physics*, 143(18):181103, 2015. doi: 10.1063/1.4935712. URL `http://dx.doi.org/10.1063/1.4935712`.

[13] J. M. Cullen and M. C. Zerner. The linked singles and doubles model: An approximate theory of electron correlation based on the coupled-cluster ansatz. *The Journal of Chemical Physics*, 77(8):4088–4109, 1982. doi: 10.1063/1.444319. URL `http://dx.doi.org/10.1063/1.444319`.

[14] N. Flocke and R. J. Bartlett. A natural linear scaling coupled-cluster method. *The Journal of Chemical Physics*, 121(22):10935–10944, 2004.

[15] I.-M. Høyvik, R. H. Myhre, and H. Koch. Correlated natural transition orbitals for core excitation energies in multilevel coupled cluster models. *The Journal of Chemical Physics*, 146(14):144109, 2017. doi: 10.1063/1.4979908. URL `http://dx.doi.org/10.1063/1.4979908`.

[16] M. in het Panhuis, R. W. Munn, and P. L. A. Popelier. Distributed polarizability analysis for para-nitroaniline and meta-nitroaniline: Functional group and charge-transfer contributions. *The Journal of Chemical Physics*, 120(24):11479–11486, 2004. doi: 10.1063/1.1752879. URL `http://dx.doi.org/10.1063/1.1752879`.

[17] F. Jensen. *Introduction to Computational Chemistry*. Wiley, 2007. ISBN 9780470058046. URL `https://books.google.no/books?id=RDIG48UcZfYC`.

[18] T. H. D. Jr. Gaussian basis sets for use in correlated molecular calculations. i. the atoms boron through neon and hydrogen. *The Journal of Chemical Physics*, 90(2):1007–1023, 1989.

[19] H. Koch, O. Christiansen, P. Jo/rgensen, A. M. S. de Merás, and T. Helgaker. The cc3 model: An iterative coupled cluster approach including connected triples. *The Journal of Chemical Physics*, 106(5):1808–1818, 1997.

[20] H. Koch, A. S. de Merás, and T. B. Pedersen. Reduced scaling in electronic structure calculations using cholesky decompositions. *The Journal of Chemical Physics*, 118 (21):9481–9484, 2003. doi: 10.1063/1.1578621. URL `http://dx.doi.org/10.1063/1.1578621`.

[21] A. Köhn and J. Olsen. Coupled-cluster with active space selected higher amplitudes: Performance of seminatural orbitals for ground and excited state calculations. *The Journal of Chemical Physics*, 125(17):174110, 2006.

[22] V. Kozich, W. Werncke, J. Dreyer, K.-W. Brzezinka, M. Rini, A. Kummrow, and T. Elsaesser. Vibrational excitation and energy redistribution after ultrafast internal conversion in 4-nitroaniline. *The Journal of Chemical Physics*, 117(2):719–726, 2002. doi: 10.1063/1.1482698. URL http://dx.doi.org/10.1063/1.1482698.

[23] W. D. Laidig, G. D. Purvis, and R. J. Bartlett. Localized orbitals in the coupled cluster singles and doubles model. *International Journal of Quantum Chemistry*, 22(S16):561–573, 1982. ISSN 1097-461X. doi: 10.1002/qua.560220848. URL http://dx.doi.org/10.1002/qua.560220848.

[24] A. V. Luzanov, A. A. Sukhorukov, and V. É. Umanskii. Application of transition density matrix for analysis of excited states. *Theoretical and Experimental Chemistry*, 10(4):354–361, 1976. ISSN 1573-935X. doi: 10.1007/BF00526670. URL http://dx.doi.org/10.1007/BF00526670.

[25] R. H. Myhre and H. Koch. The multilevel cc3 coupled cluster model. *The Journal of Chemical Physics*, 145(4):044111, 2016.

[26] J. Olsen. The initial implementation and applications of a general active space coupled cluster method. *The Journal of Chemical Physics*, 113(17):7140–7148, 2000.

[27] T. Owen. *Fundamentals of UV-visible Spectroscopy: A Primer*. Hewlett Packard, 1996. URL https://books.google.no/books?id=TyC7SgAACAAJ.

[28] F. Pavošević, P. Pinski, C. Riplinger, F. Neese, and E. F. Valeev. Sparsemaps—a systematic infrastructure for reduced-scaling electronic structure methods. iv. linear-scaling second-order explicitly correlated energy with pair natural orbitals. *The Journal of Chemical Physics*, 144(14):144109, 2016. doi: 10.1063/1.4945444. URL http://dx.doi.org/10.1063/1.4945444.

[29] J. A. Pople, R. Krishnan, H. B. Schlegel, and J. S. Binkley. Electron correlation theories and their application to the study of simple reaction potential surfaces. *International*

*Journal of Quantum Chemistry*, 14(5):545–560, 1978. ISSN 1097-461X. doi: 10.1002/qua.560140503. URL http://dx.doi.org/10.1002/qua.560140503.

[30] A. M. J. S. d. M. R. H. Myhre and H. Koch. Multi-level coupled cluster theory. *The Journal of Chemical Physics*, 141(22):224105, 2014.

[31] S. Saebø and P. Pulay. Local treatment of electron correlation. *Annual Review of Physical Chemistry*, 44(1):213–236, 1993.

[32] M. Schütz and H.-J. Werner. Low-order scaling local electron correlation methods. iv. linear scaling local coupled-cluster (lccsd). *The Journal of Chemical Physics*, 114(2): 661–681, 2001.

[33] Y. Shao, Z. Gan, E. Epifanovsky, A. T. Gilbert, M. Wormit, J. Kussmann, A. W. Lange, A. Behn, J. Deng, X. Feng, D. Ghosh, M. Goldey, P. R. Horn, L. D. Jacobson, I. Kaliman, R. Z. Khaliullin, T. Kuś, A. Landau, J. Liu, E. I. Proynov, Y. M. Rhee, R. M. Richard, M. A. Rohrdanz, R. P. Steele, E. J. Sundstrom, H. L. W. III, P. M. Zimmerman, D. Zuev, B. Albrecht, E. Alguire, B. Austin, G. J. O. Beran, Y. A. Bernard, E. Berquist, K. Brandhorst, K. B. Bravaya, S. T. Brown, D. Casanova, C.-M. Chang, Y. Chen, S. H. Chien, K. D. Closser, D. L. Crittenden, M. Diedenhofen, R. A. D. Jr., H. Do, A. D. Dutoi, R. G. Edgar, S. Fatehi, L. Fusti-Molnar, A. Ghysels, A. Golubeva-Zadorozhnaya, J. Gomes, M. W. Hanson-Heine, P. H. Harbach, A. W. Hauser, E. G. Hohenstein, Z. C. Holden, T.-C. Jagau, H. Ji, B. Kaduk, K. Khistyaev, J. Kim, J. Kim, R. A. King, P. Klunzinger, D. Kosenkov, T. Kowalczyk, C. M. Krauter, K. U. Lao, A. D. Laurent, K. V. Lawler, S. V. Levchenko, C. Y. Lin, F. Liu, E. Livshits, R. C. Lochan, A. Luenser, P. Manohar, S. F. Manzer, S.-P. Mao, N. Mardirossian, A. V. Marenich, S. A. Maurer, N. J. Mayhall, E. Neuscamman, C. M. Oana, R. Olivares-Amaya, D. P. O'Neill, J. A. Parkhill, T. M. Perrine, R. Peverati, A. Prociuk, D. R. Rehn, E. Rosta, N. J. Russ, S. M. Sharada, S. Sharma, D. W. Small, A. Sodt, T. Stein, D. Stück, Y.-C. Su, A. J. Thom, T. Tsuchimochi, V. Vanovschi, L. Vogt, O. Vydrov, T. Wang, M. A. Watson, J. Wenzel, A. White, C. F. Williams, J. Yang, S. Yeganeh, S. R. Yost, Z.-Q. You, I. Y. Zhang,

X. Zhang, Y. Zhao, B. R. Brooks, G. K. Chan, D. M. Chipman, C. J. Cramer, W. A. G. III, M. S. Gordon, W. J. Hehre, A. Klamt, H. F. S. III, M. W. Schmidt, C. D. Sherrill, D. G. Truhlar, A. Warshel, X. Xu, A. Aspuru-Guzik, R. Baer, A. T. Bell, N. A. Besley, J.-D. Chai, A. Dreuw, B. D. Dunietz, T. R. Furlani, S. R. Gwaltney, C.-P. Hsu, Y. Jung, J. Kong, D. S. Lambrecht, W. Liang, C. Ochsenfeld, V. A. Rassolov, L. V. Slipchenko, J. E. Subotnik, T. V. Voorhis, J. M. Herbert, A. I. Krylov, P. M. Gill, and M. Head-Gordon. Advances in molecular quantum chemistry contained in the q-chem 4 program package. *Molecular Physics*, 113(2):184–215, 2015. doi: 10.1080/00268976.2014.952696. URL `http://dx.doi.org/10.1080/00268976.2014.952696`.

[34] J. E. Subotnik and M. Head-Gordon. A local correlation model that yields intrinsically smooth potential-energy surfaces. *The Journal of Chemical Physics*, 123(6):064108, 2005.

[35] P. J. T. Helgaker and J. Olsen. *Molecular Electronic-Structure Theory*. John Wiley & Sons, 2000.

[36] H.-M. Xiao, X.-H. Ju, L.-N. Xu, and G.-Y. Fang. A density-functional theory investigation of 3-nitro-1,2,4-triazole-5-one dimers and crystal. *The Journal of Chemical Physics*, 121(24):12523–12531, 2004. doi: 10.1063/1.1812258. URL `http://aip.scitation.org/doi/abs/10.1063/1.1812258`.

[37] B. Yuan, Z. Yu, and E. R. Bernstein. Initial decomposition mechanism for the energy release from electronically excited energetic materials: Fox-7 (1,1-diamino-2,2-dinitroethene, c2h4n4o4). *The Journal of Chemical Physics*, 140(7):074708, 2014. doi: 10.1063/1.4865266. URL `http://dx.doi.org/10.1063/1.4865266`.